Geophysical Research Letters

RESEARCH LETTER
10.1002/2018GL077656

Special Section:
Cassini's Final Year: Science Highlights and Discoveries

Energetic Electron Pitch Angle Distributions During the Cassini Final Orbits

J. F. Carbary[1], D. G. Mitchell[1], P. Kollmann[1], N. Krupp[2], E. Roussos[2], and M. K. Dougherty[3]

[1]Johns Hopkins University Applied Physics Laboratory, Laurel, MD, USA, [2]Max-Planck-Institute für Sonnensystemforschung, Göttingen, Germany, [3]Blackett Laboratory, Imperial College, London, UK

Key Points:
- Energetic electrons (110–365 keV) move *away* from Saturn along field lines outside Titan's *L*-shell, indicating open field lines
- Bidirectional and pancake distributions exist inside the *L*-shell of Titan, indicating closed field lines
- Thus, Titan's *L*-shell is an approximate boundary for open/closed field lines

Correspondence to:
J. F. Carbary,
james.carbary@jhuapl.edu

Citation:
Carbary, J. F., Mitchell, D. G., Kollmann, P., Krupp, N., Roussos, E., & Dougherty, M. K. (2018). Energetic electron pitch angle distributions during the Cassini final orbits. *Geophysical Research Letters*, *45*, 2911–2917. https://doi.org/10.1002/2018GL077656

Received 22 FEB 2018
Accepted 20 MAR 2018
Accepted article online 26 MAR 2018
Published online 13 APR 2018

©2018. American Geophysical Union. All Rights Reserved.

Abstract Pitch angle distributions (PADs) of very energetic electrons (110–365 keV) are examined during the ring-grazing and proximal orbits of the Cassini spacecraft, from day 320 2016 (15 November) to day 257 2017 (14 September). These repeating orbits allowed a statistical evaluation of the PADs within the magnetopause on the nightside of Saturn. Along *L*-shells (i.e., equatorial crossing distances of magnetic field lines) near and outside that of Titan and north of the equator, the electron fluxes were unidirectionally field-aligned going *away* from Saturn. Along *L*-shells inside Titan's and south of the equator, the electrons had bidirectional or pancake (trapping) PADs. This behavior suggests that the field lines within Titan's *L*-shell are generally closed, while those outside of that *L*-shell are generally open. This result strictly applies only to the nightside local times sampled during the final Cassini orbits, but one may infer a similar behavior at other times.

Plain Language Summary The angle between the magnetic field vector and the velocity of an electron is known as the pitch angle. Sufficiently energetic electrons move at essentially the speed of light, so they can effectively sample the entire length of a magnetic field line. Therefore, the pitch angle distributions of energetic electron fluxes can serve as an indicator of whether the field line is open (i.e., electrons at pitch angles of 0° or 180°) or closed (i.e., electrons at pitch angles of 0° and 180° or at pitch angles of 90°). The pitch angle distributions of electrons during the final orbits of Cassini indicate the field lines are closed inside the magnetic shell of the moon Titan and open outside this shell. This finding has important implications for the global topology of Saturn's magnetic field.

1. Introduction

Energetic electron pitch angle distributions (PADs) can identify open and closed magnetic field lines in a planetary magnetosphere. A distribution that peaks near 90° indicates the local field line is closed, and such a distribution is commonly referred to as a "trapping" or "pancake" distribution. In a trapping distribution, particles are confined closely to a minimum in the magnetic field strength. A distribution having two maxima near 0° and 180° also indicates the field line is closed because the particles "bounce" between two mirror points, one at each end of a converging field. Such a distribution is called a "cigar" or, more appropriately, a "bidirectional" distribution. Both the pancake and the bidirectional distributions represent mirroring populations, albeit the former mirror at the equator and the latter at the field line feet. A distribution with one maximum near 0° or one near 180° indicates an open field line because the particles are moving in one direction only and are not mirroring at the ends of a field line. Such a distribution is called "unidirectional." Because energetic electrons move so quickly, these distributions are usually regarded as instantaneous indicators of the magnetic field configuration.

The PADs of energetic electrons have served to delineate magnetospheric boundaries and accelerations regions at Earth, Jupiter, and Saturn (see Carbary et al. (2011) for a summary of such research). Several investigations relevant to the present study have described the electron PADs in Saturn's magnetosphere. Bidirectional and trapping distributions of energetic electrons were first measured in Saturn's magnetosphere by Pioneer 11 instruments in 1979 (e.g., Van Allen, Randall, & Thomsen, 1980), and similar measurements were made by instruments during the Voyager 1 and 2 flybys (e.g., Krimigis et al., 1983).

The 13-year mission of Cassini at Saturn provided the first long-term measurements of electron PADs at Saturn. The Low Energy Magnetospheric Measurement System (LEMMS) of the Magnetospheric Imaging System (MIMI) has monitored energetic electrons throughout the Cassini mission (Krimigis et al., 2004).

Strong bidirectional distributions of energetic electrons were first observed during the early orbits of Cassini about Saturn, and such distributions were associated with acceleration in the planet's aurora (Saur et al., 2006). Bidirectional PADs of energetic electrons are commonly observed outside of L~10 R_S (1 R_S = 60,268 km) and most often on the nightside, with trapping distributions in the inner magnetosphere (Carbary et al., 2011; Krupp et al., 2009). Clark et al. (2014) extended this work by providing a complete summary of energetic electron PADs from 2004 to 2012. Within quasiperiodic events (called "QP60 events" wherein fluxes have periods of ~60 min), the PADs are likely to have strongly bidirectional distributions and may be associated with certain plasma wave and magnetic field fluctuations (Palmaerts et al., 2016; Roussos et al., 2016). A plasmasphere-like boundary, detected at high latitudes using Langmuir probe and plasma wave data, was associated with a change in the PADs of energetic electrons, signaling open magnetic field lines on the poleward side of this boundary (Gurnett et al., 2010). Ion conics and field-aligned electron beams are associated with auroral processes at Saturn (Mitchell et al., 2009). Case studies indicate that these electron beams can be either unidirectional or bidirectional. Energetic electron PADs were used in conjunction with other Cassini instruments to determine Saturn's polar cap boundary, mapped to the ionosphere, for 2004–2009 (Jinks et al., 2014). Both high and low energy ion and electron beams have been related to infrared auroral arcs at Saturn in association with transient reconnection events (Badman et al., 2012).

Similar investigations have been conducted for the lower energy electrons ($E < 3$ keV) using the Cassini Plasma Spectrometer (CAPS; Young et al., 2004). Such electrons also exhibit bidirectional structures, and these are sometimes associated with field-aligned currents inferred from magnetometer measurements or with an instability region associated with Saturn kilometric radiation (Schippers et al., 2011, 2012). A study of 12 to 100-eV electrons showed that field-aligned electrons were more closely linked with interchange processes than trapped electrons (DeJong et al., 2010). A statistical examination of the low energy electron PADs throughout the Cassini mission reveals a global structure similar to that of the energetic electrons, with trapping distributions at low L-shells and bidirectional distributions at high L-shells (Carbary & Rymer, 2014). A unidirectional upward flux in the low-energy electrons (hundreds of eV in energy) has been reported using CAPS observations, and such a beam was associated with the generation of auroral hiss at high latitudes via the growth of whistler mode waves (Kopf et al., 2010).

The final ~44 ring-grazing and proximal orbits of Cassini offer a somewhat different perspective on the electron PADs. These orbits repeated for the last ~300 days of the mission when Cassini's periapsis came closer to the planet, first just outside, and then inside the main rings. All these final orbits were on the nightside near midnight and covered a wide range of magnetic L-shells at high northern and southern latitudes. Cassini not only sampled the rings and radiation belts but also the auroral, polar cap, magnetic lobe, and magnetotail regions. Because the CAPS instrument failed earlier in the mission, the PADs of low energy electrons are unavailable during the "Grand Finale" orbits. However, LEMMS did provide frequent measurements of energetic electron PADs during the last orbits. A statistical examination of these PADs can reveal the location of the open/closed field line boundary in Saturn's magnetosphere.

2. Instrument and Data Set

This investigation discusses PADs from mildly relativistic electrons measured by the MIMI/LEMMS detector. This detector was mounted on a turntable to enable scanning through pitch angles, but the turntable failed in early 2005. Since then, LEMMS has relied on roll maneuvers of the Cassini spacecraft to sample pitch angles. Thus, the PAD coverage by LEMMS was not continuous during the mission. However, Cassini frequently executed rolls during the Grand Finale orbits, often rolling continuously for several hours per day, and pitch angle coverage was greatly enhanced. Unfortunately, the rolls did not always scan a full 180° in pitch angle. To achieve good statistics and optimize pitch angle coverage, this investigation only employs rolls that covered 120° or more in pitch angle.

Pitch angle coverage can be further enhanced by using the double-ended feature of the LEMMS detector. LEMMS consists of a set of low-energy electron "C" detectors (the low energy telescope, LET) looking in the "forward" direction of the instrument complemented by a set of high-energy "E" detectors (the high energy telescope, HET) looking in the "backward" direction 180° away. Several of the LET C channels overlap in energy the lowest energy HET E0 channel (110–365 keV), so that the fluxes of three C channels can be combined to be equivalent to the E0 channel, called E0*,

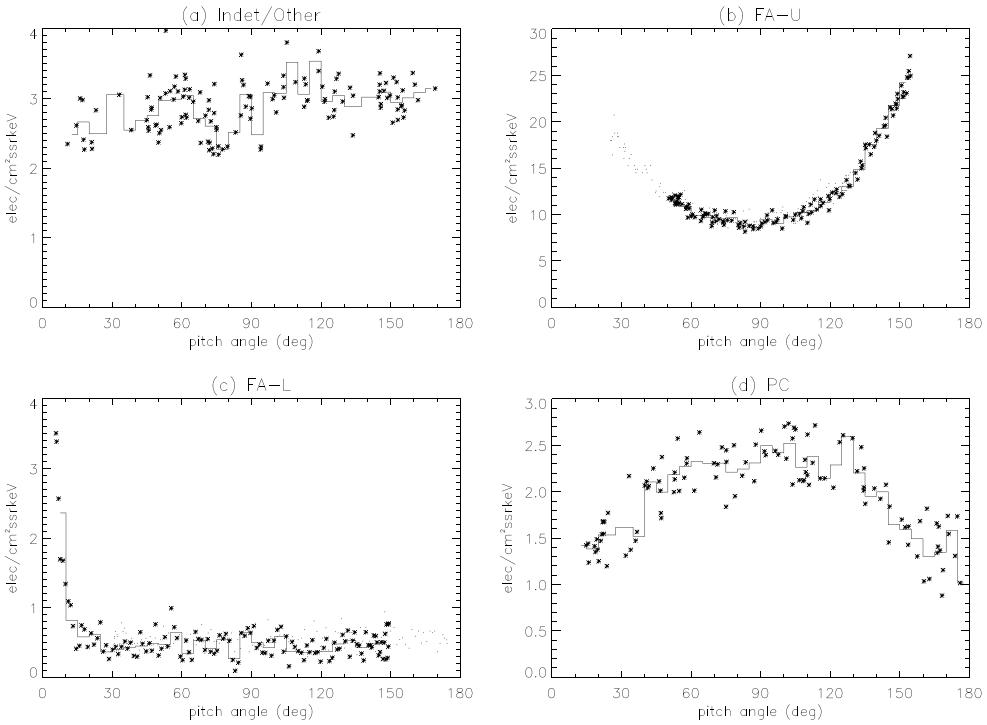

Figure 1. Classifying the various pitch angle distributions (PADs) observed during the F-ring and proximal orbits of Cassini. Pitch angles were sampled by rotational maneuvers of the Cassini spacecraft, which occurred frequently during the Grand Finale orbits. Only PADs for which over 120° of pitch angle were included in the statistics. Generally, most of the PADs were of the "indeterminate" or "other" type shown in (a). Less frequent were the bidirectional field-aligned ("U" shape) distributions typical of that shown in (b) and the unidirectional ("L" shape) distributions in (c) either parallel or antiparallel to the magnetic field. (d) Relatively rare pancake (trapping) distribution with a peak near 90°. In all panels, a histogram indicates averages in 5° pitch angle bins. The E0* fluxes are indicated as asterisks in all the panels, while the complementary E0 fluxes are shown as dots in (b) and (c).

$$E0^{*} = 0.1{\cdot}C4 + 0.5{\cdot}C5 - 0.25{\cdot}C7 \approx E0 \quad (1)$$

where C4, C5, and C7 refer to the fluxes in those forward LET channels, while E0 is the flux in the single backward HET channel. This combination of C channels is called the E0* channel, which is approximately equivalent to the E0 channel. The various constants in (1) adjust for the energy response and efficiency between the E0* and E0 channels. Equation (1) has been found to be valid for radial distances $r > 4\ R_S$. Inside this radial distance, the electron channels suffer from contamination from penetrating energetic protons, and a different set of constants must be used. The observations discussed here were obtained outside the radiation belts (L ~4). Standard MIMI data processing is used to compute the fluxes of the E0* and E0 electron channels (e.g., Krimigis et al., 2004). The fluxes have a time resolution of ~5 s, which is much less than the typical time of one pitch angle scan of ~10^2 s. Note that electrons with E0 energies travel ~100 R_S in ~30 s.

The pitch angle α_* of the E0* channels is the angle between the LEMMS antiboresight (at its "fixed" position) and the magnetic field. The magnetic field was provided by the Cassini Magnetometer experiment (Dougherty et al., 2004), appropriately averaged within the sampling time of LEMMS. Thus, α_* refers to the direction of motion of the electrons, not to their angle of incidence. To clarify, α_* represents the angle between the magnetic field and the instantaneous velocity vector of the electron. Because the E0 channel looked in the opposite direction of the E0* channel, its pitch angles are $\alpha_0 = 180° - \alpha_*$. The pitch angle $\Delta\alpha$ coverage for one roll is determined by MAX$\{|\alpha_* - \alpha_0|\}$. Here $\Delta\alpha > 120°$. Both the E0* and E0 channels were examined in determining the type of the PAD.

3. Types of PADs

Several distinct types of PAD appeared during the Grand Finale orbits, and these are displayed in Figure 1. Each type of PAD has an easily recognized appearance. The most common of these distributions (Figure 1a) did not resemble a unidirectional, bidirectional, or pancake distribution and was therefore classified as

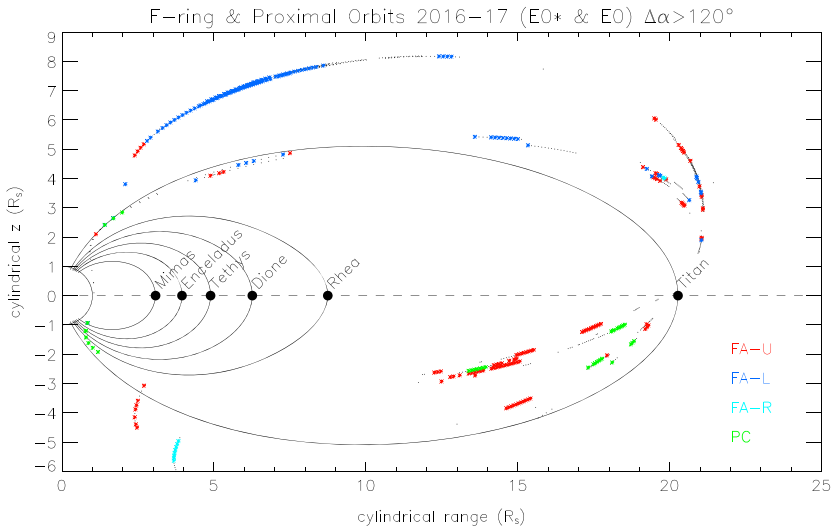

Figure 2. Locations of different types of pitch angle distributions (PADs) during the F-ring and proximal orbits. The black dots represent pitch angle scans that sampled 120° or more in pitch angle. The dark blue asterisks indicate unidirectional field-aligned PADs (FA-L), while the light blue asterisks show unidirectional antifield-aligned PADs (FA-R). Both blue colors indicate fluxes away from Saturn. The red asterisks indicate bidirectional field-aligned PADs (FA-U). The green asterisks indicate pancake distributions (PC). The PAD pattern is striking. The unidirectional PADs occur predominately in the north along or outside of the *L*-shell associated with Titan. The bidirectional and pancake PADs occur predominately in the south within the *L*-shell of Titan. The *L*-shells of the several moons were determined using the magnetic field model of Achilleos et al. (2010).

"indeterminate" or "other." Occasionally, some coherent distribution such as a "butterfly" would occur (i.e., dual peaks with one between 0°–90° and another between 90°–180°) in the indeterminates/others, but usually, the distribution was simply not recognizable. Distributions in the indeterminate/other category were excluded if the median flux was less than three times the E0 background, which is meant to remove very low flux distributions with poor statistics. A common distribution was the bidirectional field-aligned PAD exemplified in Figure 1b. This distribution was recognized earlier in energetic electrons (Carbary et al., 2011; Clark et al., 2014; Saur et al., 2006) and is common in the outer magnetosphere. Such a PAD will be denoted as "FA-U" in this paper. The unidirectional distribution of Figure 1c has been remarked upon in studies of ion conics and a plasmasphere-like boundary (Gurnett et al., 2010; Mitchell et al., 2009). Figure 1c shows a "left-hand" unidirectional field-aligned distribution in which the fluxes are moving along the field line. This PAD is denoted "FA-L" here. Rarely, a "right-hand unidirectional PAD is observed; this is referred to as "FA-R" and signifies a unidirectional distribution in which the fluxes are antiparallel to the field line. Finally, Figure 1d shows a typical pancake or trapping distribution, here denoted simply as "PC." As discussed below, the abundance of FA-L distributions and the paucity of FA-R distributions have to do with the spacecraft location, and both represent fluxes moving away from Saturn on open field lines.

The several types of PADs were determined by manual inspection of all the PADs for which $\Delta\alpha > 120°$ from day 320 2006 to day 257 2017. There were a total of 575 such pitch angle scans during this time interval. In many cases, the bidirectional and unidirectional PADs were extremely field-aligned, with fluxes at background levels for pitch angles not within a few degrees of 0° or 180°. Figure 1c shows an example of such extreme field alignment. This study makes no effort to quantify this unidirectional structure, although these distributions are associated with ion conics and auroral phenomena (e.g., Mitchell et al., 2009).

4. Locations of the Distributions

Figure 2 locates the various PAD types in cylindrical coordinates where the origin is at the center of Saturn. A consistent pattern emerges. Unidirectional PADs (dark blue and light blue) occur predominately in the northern lobe outside of Titan's *L*-shell. Bidirectional (red) and pancake (green) PADs appear in the south inside of Titan's *L*-shell. PADs immediately north of Titan at ~20 R_S have a mix of different kinds of PADS. This behavior suggests that the open-closed boundary varies considerably in that region of the magnetosphere. That is, sometimes these field lines are open and sometimes closed, and the field configuration in this region is dynamically variable, probably due to mechanisms mentioned in the

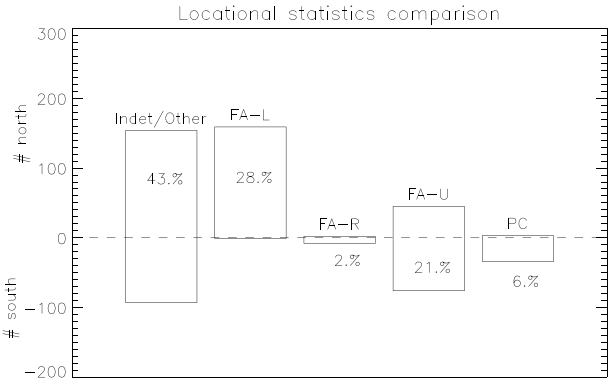

Figure 3. Statistical distribution of the various PADs, segregated into northern and southern branches. Note that most of the distributions are indeterminate, meaning they are not unidirectional, bidirectional, or pancake. The indeterminate/other category represents distributions that could not be fit into the other categories, and for which the median flux was above three times the E0 background. The total number of pitch angle distributions of all categories was 575.

introduction. This pattern suggests that, outside of Titan's *L* shell, the high-latitude field lines in the magnetic lobes are open, while those at lower latitudes may be dynamically closed or open and that all field lines inside of Titan's *L* shell are definitely closed. In the context of energetic electron PADS, this represents a global delineation of the magnetic field topology at Saturn, which agrees well with the force-balance model of Achilleos, Guio, and Arridge (2010). (Here *L*-shell means the equatorial crossing distance of a magnetic field line, not necessarily a dipole field line.)

The outlier PADs in Figure 2 also merit interest. In the lower left of the figure at a latitude of ~45°, several antifield aligned PADs appear (light blue), as well as several bidirectional PADs at closer ranges (red), and trapping distributions (green) very close to the planet. This arrangement suggests that electron outflow occurs in the southern lobes as well as the northern and that field lines are indeed closed very near the planet. A few bidirectional and pancake distributions also appear at high northern latitudes close to Saturn. The former may represent some sort of acceleration region, while the pancake PADs may suggest a possible trapping region associated with Saturn's cusp. Note that the opening angles for the LEMMS detectors are not sufficient to resolve the loss cone except very close to the planet.

Figure 3 indicates the statistical distributions of the several PAD types and delineates these into northern and southern components. The largest number of PADs is in the indeterminate/other group, although the numbers of the other groups added together exceed the number in this group. The next-largest group are unidirectional PADs indicating movement along the field predominantly in the northern lobe. Bidirectional PADs comprise the next largest group, and these closed-field signatures are observed in both the north and the south. Pancake (trapping) distributions are also seen in both the north and the south. The few unidirectional PADs that indicate movement antiparallel to the field are mostly in the south and indicate that outflow also occurs on open lines in the south. That is, both the northern and southern unidirectional PADs represent electrons moving away from the planet on open field lines. Quite likely, more antiparallel beams would have been observed the spacecraft trajectory been more accommodating to southern exposure outside of Titan's *L*-shell (see Figure 2). The numerical distributions have purposely been left unnormalized so this spacecraft trajectory bias (north versus south) can be appreciated.

5. Discussion

Perhaps unsurprisingly, PADs from Cassini's final orbits indicate that field lines in Saturn's lobes are open in both the north and south. The open-closed boundary seems to lie somewhere near or outside the *L*-shell of Titan, at least on the nightside where these measurements were obtained. The exact demarcation of this boundary depends, of course, on the magnetic field model employed. The model used here is that of Achilleos et al. (2010), which is an axisymmetric force-balance model valid for typical solar wind conditions. Figure 2 suggests that nearer to the equator as well at Titan radial distances, a mixture of open and closed fields can occur. This apparent mixing may result from time-variable events such as substorms, injections, or dipolarizations that release plasmoids down the tail (e.g., Jackman et al., 2015; Mitchell et al., 2005). At any rate, the outer boundary of the open/closed region is apparently dynamic.

The inner (or lower) boundary may or may not be dynamic—there are just not enough measurements to say. The open boundary indicated by the high-latitude passes in Figure 3 certainly lies outside the plasmapause noted by Gurnett et al. (2010), and the open field lines probably map to Saturn's polar cap. Using the model field of Achilleos et al. (2010), the *L*-shell of Titan would intersect the ionosphere at a co-latitude of ~17° (this calculation is based on a Runge-Kutta extension of the model field to an 1,100-km altitude above Saturn's standard ellipsoid as given in Carbary et al. (2010)). Thus, the open-closed boundary must lie at latitudes poleward of ~17°, which agree with the determination of the polar cap boundaries of 15.6° (south) and 13.3° (north) made by Jinks et al. (2014).

As exemplified in Figure 1c, many of these unidirectional PADs are extremely field aligned and are essentially electron beams moving along the field away from Saturn. As pointed out by Saur et al. (2006) and discussed

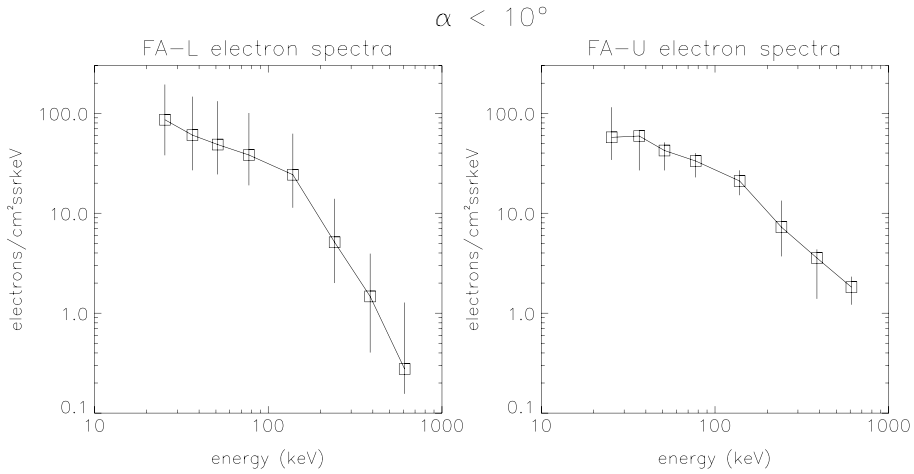

Figure 4. Median pitch angle distributions for all (left) FA-L unidirectional distributions and all (right) FA-U bidirectional distributions, obtained for pitch angles within 10° of the magnetic field. Uncertainties represent upper and lower quartiles.

at length in Mitchell et al. (2009), such parallel beams of energetic electrons are associated with Saturn's aurora. Field-aligned electron beams and upgoing ion fluxes can be generated by a "pressure-cooker" potential that generates field-aligned ions once they are accelerated in the potential to the sufficient energies. Field-aligned electrons are associated with a downward current drawn by magnetospheric conditions that generate the potential. A similar model has been advocated to explain the ion conics and field-aligned electrons at Earth (e.g., Carlson et al., 1998) and has been used to explain similar phenomena at Saturn (Mitchell et al., 2009).

These PADs of Saturn's energetic electrons also resemble the unidirectional and bidirectional distributions recently detected at similar energies by the JEDI instrument on the Juno spacecraft at Jupiter (Mauk et al., 2017b, 2017a). In some instances, the Jovian spectra exhibit a peak and/or cutoff in their energy spectra that indicate a field-aligned potential. At other times, there are no peaks and no cutoffs in the spectra. Figure 4 illustrates the combined spectra for Saturn's unidirectional and bidirectional spectra, shown as medians obtained for pitch angles within 10° of the magnetic field. While no peak appears in either spectrum, there is a noticeable discontinuity near ~110 keV in the FA-L spectrum. This could conceivably indicate a field-aligned potential, one that directs the electrons outwards along the field line rather than downwards toward the ionosphere.

6. Conclusions

The PADs of energetic electrons (110–365 keV) are surveyed during the final orbits of Cassini. Field-aligned, unidirectional distributions exist north and south of the equator outside the *L*-shell of Titan, indicating open field lines, while bidirectional and pancake distributions are seen south of the equator inside the *L*-shell of Titan, indicating closed field lines. This observation describes the statistical location of open and closed field lines in Saturn's magnetosphere, although only for the nightside sampling of the final orbits.

Acknowledgments
The data reported herein from MIMI/LEMMS are or will be available through the NASA Planetary Data Center under the Cassini Programs at the website pds.jpl.nasa.gov. This research was supported by the NASA Office of Space Science under Task Order 003 of contract NAS5-97271 between NASA Goddard Space Flight Center and the Johns Hopkins University.

References

Achilleos, N., Guio, P., & Arridge, C. S. (2010). A model of force balance in Saturn's magnetodisc. *Monthly Notices of the Royal Astronomical Society*, *401*(4), 2349–2371. https://doi.org/10.1111/j.1365-2966.2009.15865.x

Badman, S. V., Achilleos, N., Arridge, C. S., Baines, K. H., Brown, R. H., Bunce, E. J., et al. (2012). Cassini observations of ion and electron beams at Saturn and their relationship to infrared auroral arcs. *Journal of Geophysical Research*, *117*, A01211. https://doi.org/10.1029/2011JA017222

Carbary, J. F., Achilleos, N., Arridge, C. S., Khurana, K. K., & Dougherty, M. K. (2010). Global configuration of Saturn's magnetic field derived from observations. *Geophysical Research Letters*, *37*, L21806. https://doi.org/10.1029/2010GL044622

Carbary, J. F., Mitchell, D. G., Paranicas, C., Roelof, E. C., Krimigis, S. M., Krupp, N., et al. (2011). Pitch angle distributions of energetic electrons at Saturn. *Journal of Geophysical Research*, *116*, A01216. https://doi.org/10.1029/2010JA015987

Carbary, J. F., & Rymer, A. M. (2014). Meridional maps of Saturn's thermal electrons. *Journal of Geophysical Research: Space Physics*, *119*, 1721–1733. https://doi.org/10.1002/2013JA019436

Carlson, C. W., McFadden, J. P., Ergun, R. E., Temerin, M., Peria, W., Mozer, F. S., et al. (1998). FAST observations in the downward auroral current regions: Energetic upgoing electron beams, parallel potential drops, and ion heating. *Geophysical Research Letters*, *25*(12), 2017–2020. https://doi.org/10.1029/98GL00851

Clark, G., Paranicas, C., Santos-Costa, D., Livi, S., Krupp, N., Mitchell, D. G., et al. (2014). Evolution of electron pitch angle distributions across Saturn's middle magnetospheric regions from MIMI/LEMMS. *Planetary and Space Science*, *104*, 18–28. https://doi.org/10.1016/j.pss.2014.07.004

DeJong, A. D., Burch, J. L., Goldstein, J., Coates, A. J., & Young, D. T. (2010). Low-energy electrons in Saturn's inner magnetosphere and their role in interchange injections. *Journal of Geophysical Research*, *115*, A10229. https://doi.org/10.1029/2010JA015510

Dougherty, M. K., Kellock, S., Southwood, D. J., Balogh, A., Smith, E. J., Tsurutani, B. T., et al. (2004). The Cassini magnetic field investigation. *Space Science Reviews*, *114*(1-4), 331–383. https://doi.org/10.1007/s11214-004-1432-2

Gurnett, D. A., Persoon, A. M., Kopf, A. J., Kurth, W. S., Morooka, M. W., Wahlund, J. E., et al. (2010). A plasmapause-like boundary at high latitudes in Saturn's magnetosphere. *Geophysical Research Letters*, *37*, L16806. https://doi.org/10.1029/2010GL044466

Jackman, C. M., Thomsen, M. F., Mitchell, D. G., Sergis, N., Arridge, C. S., Felici, M., et al. (2015). Field dipolarization in Saturn's magnetotail with planetward ion flows and energetic particle flow bursts: Evidence of quasi-steady reconnection. *Journal of Geophysical Research: Space Physics*, *120*, 3603–3617. https://doi.org/10.1002/2015JA020995

Jinks, S. L., Bunce, E. J., Cowley, S. W. H., Provan, G., Yeoman, T. K., Arridge, C. S., et al. (2014). Cassini multi-instrument assessment of Saturn's polar cap boundary. *Journal of Geophysical Research: Space Physics*, *119*, 8161–8177. https://doi.org/10.1002/2014JA020367

Kopf, A. J., Gurnett, D. A., Menietti, J. D., Schippers, P., Arridge, C. S., Hospodarsky, G. B., et al. (2010). Electron beams as the source of whistler-mode auroral hiss at Saturn. *Geophysical Research Letters*, *37*, L09102. https://doi.org/10.1029/2010GL042980

Krimigis, S. M., Carbary, J. F., Keath, E. P., Armstrong, T. P., Lanzerotti, L. J., & Gloeckler, G. (1983). General characteristics of hot plasma and energetic particles in the Saturnian magnetosphere: Results from the Voyager spacecraft. *Journal of Geophysical Research*, *88*(A11), 8871–8892. https://doi.org/10.1029/JA088iA11p08871

Krimigis, S. M., Mitchell, D. G., Hamilton, D. C., Livi, S., Dandouras, J., Jaskulek, S., et al. (2004). Magnetospheric Imaging Instrument (MIMI) on the Cassini mission to Saturn/Titan. *Space Science Reviews*, *114*(1-4), 233–329. https://doi.org/10.1007/s11214-004-1410-8

Krupp, N., Roussos, E., Lagg, A., Woch, J., Müller, A. L., Krimigis, S. M., et al. (2009). Energetic particles in Saturn's magnetosphere during the Cassini nominal mission (July 2004–July 2008). *Planetary and Space Science*, *57*(14-15), 1754–1768. https://doi.org/10.1016/j.pss.2009.06.010

Mauk, B. H., Haggerty, D. K., Paranicas, C., Clark, G., Kollmann, P., Rymer, A. M., et al. (2017a). Discrete and broadband electron acceleration ion Jupiter's powerful aurora. *Nature*, *549*(7670), 66–69. https://doi.org/10.1038/nature23648

Mauk, B. H., Haggerty, D. K., Paranicas, C., Clark, G., Kollmann, P., Rymer, A. M., et al. (2017b). Juno observations of energetic charged particles over Jupiter's polar regions: Analysis of monodirectional and bidirectional electron beams. *Geophysical Research Letters*, *44*, 4410–4418. https://doi.org/10.1002/2016GL072286

Mitchell, D. G., Brandt, P. C., Roelof, E. C., Dandouras, J., Krimigis, S. M., Mauk, B. H., et al. (2005). Energetic ion acceleration in Saturn's magnetotail: Substorms at Saturn? *Geophysical Research Letters*, *32*, L20S01. https://doi.org/10.1029/2005GL022647

Mitchell, D. G., Kurth, W. S., Hospodarsky, G. B., Krupp, N., Saur, J., Mauk, B. H., et al. (2009). Ion conics and electron beams associated with auroral processes on Saturn. *Journal of Geophysical Research*, *114*, A02212. https://doi.org/10.1029/2008JA013621

Palmaerts, B., Roussos, E., Krupp, N., Kurth, W. S., Mitchell, D. G., & Yates, J. N. (2016). Statistical analysis and multi-instrument overview of the quasi-periodic 1-hour pulsations in Saturn's outer magnetosphere. *Icarus*, *271*, 1–18. https://doi.org/10.1016/j.icarus.2016.01.025

Roussos, E., Krupp, N., Mitchell, D. G., Paranicas, C., Krimigis, S. M., Andriopoulou, M., et al. (2016). Quasi-periodic injections of relativistic electrons in Saturn's outer magnetosphere. *Icarus*, *263*, 101–116. https://doi.org/10.1016/j.icarus.2015.04.017

Saur, J., Mauk, B. H., Mitchell, D. G., Krupp, N., Khurana, K. K., Livi, S., et al. (2006). Anti-planetward auroral electron beams at Saturn. *Nature*, *439*(7077), 699–702. https://doi.org/10.1038/nature04401

Schippers, P., André, N., Gurnett, D. A., Lewis, G. R., Persoon, A. M., & Coates, A. J. (2012). Identification of electron field-aligned current systems in Saturn's magnetosphere. *Journal of Geophysical Research*, *117*, A05204. https://doi.org/10.1029/2011JA017352

Schippers, P., Arridge, C. S., Menietti, J. D., Gurnett, D. A., Lamy, L., Cecconi, B., et al. (2011). Auroral electron distributions within and close to the Saturn kilometric radiation source region. *Journal of Geophysical Research*, *116*, A05203. https://doi.org/10.1029/2011JA016461

Van Allen, J. A., Randall, B. A., & Thomsen, M. F. (1980). Sources and sinks of energetic electrons and protons in Saturn's magnetosphere. *Journal of Geophysical Research*, *85*(A11), 5679–5694. https://doi.org/10.1029/JA085iA11p05679

Young, D. T., Berthelier, J. J., Blanc, M., Burch, J. L., Coates, A. J., Goldstein, R., et al. (2004). Cassini Plasma Spectrometer investigation. *Space Science Reviews*, *114*(1-4), 1–112. https://doi.org/10.1007/s11214-004-1406-4